

## 尺度空間の階層構造に基づく動画像の時間分割

酒井 智弥<sup>†</sup> 井宮 淳<sup>†</sup>

<sup>†</sup> 千葉大学総合メディア基盤センター

あらまし 動画像中の物体の階層構造の推移に基づく時間分割法を提案する．また，その応用として心臓動画の時間分割を示す．提案手法は動画像中の物体の定性的な構造変化を検出するため，物体の形状や動きを定量的に評価することなく時間分割を実現している．本稿では，図流線，特異点と停留点の接続性，無限遠点といった新しい概念を尺度空間解析に導入し，異なる尺度（または解像度）における画像の特徴点の階層的な相互関係を明確に定義している．

## Temporal Segmentation of Motion Image Based on Scale-Space Hierarchy

Tomoya SAKAI<sup>†</sup> and Atsushi IMIYA<sup>†</sup>

<sup>†</sup>Institute of Media and Information Technology, Chiba University

**Abstract** Objects in motion image change their structure. This article proposes a temporal segmentation scheme based on the transitions of the hierarchical structure of frame images. A segmentation of heart motion is shown as a potential application. The hierarchical structure is presented by the Gaussian scale-space, in which tracks of image feature points across scale represent interrelationships between them. In order to clarify the scale-space hierarchy, we introduce some novel concepts for consistency: figure field, connectivity of singular points and stationary points of image intensity, including a local minimum point at infinity.

### 1 Introduction

The aim of this article is to develop a method to divide a motion image into temporal segments by detecting structural transitions of objects in the image. We apply the scale-space analysis [1, 2, 3, 4, 5], which treats the images at all levels of resolution, simultaneously. Generally, the resolution of the image governs stability, accuracy and cost of quantitative estimations such as edge extractions or motion detections of the objects. Therefore, we require a priori knowledge of necessary and sufficient resolution to employ the quantitative estimations. That is, the scale selection problem is inevitable.

The scale-space analysis allows us to avoid the quantitative estimations in the temporal segmentation. We can instead obtain qualitative description of image structure, i.e. the scale-space hierarchy. Firstly, we introduce the scale-space theory and define the scale-space tree, which describes the hierarchical structure of image at fixed time. Secondly, we define the temporal tree as a sequence of scale-space trees for the motion image. We demonstrate the temporal segmentation of beating heart without any a priori knowledge.

### 2 Gaussian Scale Space

#### 2.1 Principle

Consider transformation of a given greyscale image  $f(\mathbf{x})$  into low-resolution images without creating spurious structures. The transformation is supposed to satisfy some fundamental principles: positivity preserving, linearity, translation invariance, scale and rotation invariance, and semigroup (associative) property. Such transformation is known as the isotropic Gaussian convolution [1, 6]. The Gaussian convolution yields a one parameter family of blurred images  $f(\mathbf{x}, \tau)$ . The parameter  $\tau > 0$  represents the scale, which is related to the width of the Gaussian kernel function. The function  $f(\mathbf{x}, \tau)$ , the Gaussian scale-space image, is the solution to the linear diffusion equation,

$$\frac{\partial}{\partial \tau} f(\mathbf{x}, \tau) = \Delta f(\mathbf{x}, \tau), \tau > 0, f(\mathbf{x}, 0) = f(\mathbf{x}). \quad (1)$$

Since the original image is simplified with continuously increasing the scale, we can hierarchically classify image features across scale.

## 2.2 Stationary Curve

A remarkable feature of the image is a set of stationary points of  $f(\mathbf{x}, \tau)$ . The stationary points and stationary curves are defined as follows [4].

**Definition 1.** *Stationary points are defined as the points where the gradient vanishes, that is,*

$$\{\mathbf{x} | \nabla f(\mathbf{x}, \tau) = \mathbf{0}\}. \quad (2)$$

**Definition 2.** *Stationary curves are the trajectories of stationary points  $\mathbf{x}(\tau)$  in the scale space.*

The stationary points of  $N$ -dimensional ( $N > 1$ ) scale-space images are classified into three types; local maximum points, local minimum points and saddle points. At the regular points where the determinant of the Hessian matrix of  $f(\mathbf{x}, \tau)$  is non-zero, the types of stationary point can be discriminated by the second derivative of  $f(\mathbf{x}, \tau)$ , that is, the second derivative test. Since the directional derivative of  $f(\mathbf{x}, \tau)$  in the direction of a unit vector  $\mathbf{n}$  is calculated as

$$\frac{df}{dn} = \mathbf{n}^\top \nabla f, \quad (3)$$

the second directional derivative of  $f(\mathbf{x}, \tau)$  can be written in the quadratic form,

$$\frac{d^2 f}{dn^2} = \mathbf{n}^\top \nabla (\mathbf{n}^\top \nabla f) = \mathbf{n}^\top \mathbf{H} \mathbf{n}, \quad (4)$$

where  $\mathbf{H}$  is the Hessian matrix of  $f(\mathbf{x}, \tau)$ . Equation (4) implies that the maximum and minimum values of the second directional derivative  $d^2 f/dn^2$  are the maximum and minimum eigenvalues  $\lambda_{\max}$  and  $\lambda_{\min}$  of  $\mathbf{H}$ , respectively.

$$\lambda_{\min} \leq \frac{d^2 f}{dn^2} \leq \lambda_{\max}. \quad (5)$$

The eigenvalues of  $\mathbf{H}$  and corresponding eigenvectors are called the principal curvatures and the principal directions, respectively. The principal curvatures are obtained by the second directional derivation in the principal directions. The function  $f(\mathbf{x}, \tau)$  is said to be convex if the second directional derivative  $d^2 f/dn^2$  is positive for any direction of  $\mathbf{n}$ . Analogously,  $f(\mathbf{x}, \tau)$  is concave for negative  $d^2 f/dn^2$ . The local maximum (minimum) points are the stationary points at the concave (convex) points. That is,  $\lambda_{\min} > 0$  at the minimum points and  $\lambda_{\max} < 0$  at the maximum points. The other stationary points are classified as the saddle points.

We denote the types of stationary points by combinations of the signs of the eigenvalues. In case of two-dimensional images, labels  $(-, -)$ ,  $(+, -)$  and  $(+, +)$  correspond to the local maximum points, saddle points, and local minimum points, respectively. Note that the stationary curves are also classified as local

maximum curves, saddle curves, and local minimum curves according to the second directional derivation in the same fashion.

Since the scale-space image  $f(\mathbf{x}, \tau)$  is a superposition of the Gaussian function, the local maximum and minimum points are representatives of dominant parts of bright objects and cavities in the image, respectively. The saddle points appear on ridge-like and trough-like structures in two-dimensional images. According to the sign of the Laplacian  $\Delta f(\mathbf{x}, \tau)$ , we can distinguish the saddle points as the ridge-like ( $\Delta f < 0$ ), trough-like ( $\Delta f > 0$ ), and balanced saddle ( $\Delta f = 0$ ) [7]. The balanced-saddle is also known as scale-space saddle [8].

Generally, the sign of the Laplacian depends on the sum of eigenvalues of  $\mathbf{H}$ :

$$\Delta f = \text{tr } \mathbf{H} = \text{tr}(\mathbf{V} \mathbf{A} \mathbf{V}^\top) = \sum_i \lambda_i, \quad (6)$$

where  $\mathbf{V}$  is the square matrix whose column vectors are eigenvectors of  $\mathbf{H}$ , and  $\mathbf{A}$  is the diagonal matrix of eigenvalues  $\lambda_i$ . Since the sum of the eigenvalues is negative (positive) at the local maximum (minimum) points, the image intensities on the local maximum (minimum) curves decrease (increase) with increasing scale. By the same token, the image intensities on the saddle curves composed of the ridge-like (trough-like) saddle points decrease (increase) with increasing scale.

The endpoints of the stationary curves are the singular points where  $\det \mathbf{H} = \prod_i \lambda_i = 0$ , that is, at least one of the eigenvalues is zero. This property implies that the local maximum/minimum curves and saddle curves share the singular points as their endpoints. The maximum (minimum) curves and ridge-like (trough-like) saddle curves can share the singular points with negative (positive) Laplacian.

## 2.3 Figure Field

We focus on the gradient field of the Gaussian scale-space image. The basic idea of the figure field and the following definitions were provided by Zhao and Iijima [5].

**Definition 3.** *Figure field  $\mathbf{F}$  is defined as the negative of the gradient vector field of the scale-space image, that is,*

$$\mathbf{F} = -\nabla f(\mathbf{x}, \tau). \quad (7)$$

**Definition 4.** *Figure flow curve is the directional flux curve of figure field.*

The following differential notation is directly obtained from Eq. (1) and (7):

$$\frac{\partial f}{\partial \tau} + \nabla^\top \mathbf{F} = 0. \quad (8)$$

Equation (8) is exactly the conservation law of image intensity. Therefore, the figure field  $\mathbf{F}$  is considered as the current density flow of image intensity.

The local maxima and local minima are start-points and end-points of the figure flow curves. It is trivial that  $\mathbf{F} = -\nabla f \neq 0$  at any point  $\mathbf{x}$  in the vicinity of an extrema, and we can draw a figure flow curve which passes through the point  $\mathbf{x}$  in the direction of  $\mathbf{F}$  unless  $\mathbf{x}$  is not the extrema itself. In the sense of the current density flow of image intensity, the local maxima, local minima and saddle points are sources, drains and confluences of the flow, respectively.

The saddle points are confluent points of two inward and two outward figure flow curves, which are called separatrices. The net field flux from a ridge-like (trough-like) saddle point is positive (negative). The balanced saddle points are divergenceless points since  $\nabla^\top \mathbf{F} = -\nabla^\top \nabla f = \Delta f = 0$ . This implies that the balanced saddle points are confluent points where inward and outward figure flow are balanced and totally cancelled out.

## 3 Hierarchy

### 3.1 Concept

As the scale parameter increases, the image is simplified and the features of the image are reduced. The number of stationary points in the diffused image  $f(\mathbf{x}, \tau)$  decreases when the different types of stationary points meet and annihilated at a singular point, and only one maximum point remains at the coarsest scale. The saddle points are always involved in the annihilations and creations of the stationary points [7, 8].

This behaviour of stationary points is described as the stationary curves in the scale space. The different types of stationary curves share the singular point as their endpoint. Some singular points are connected by the stationary curves to the other singular point in higher scale. Therefore, the stationary curves imply the hierarchical relationship between singular points across scale.

In order to express this implicit hierarchy as a tree, we regard the singular points as nodes of the tree. The leaves of the tree are the stationary points at the finest scale. The branches represent the connections by the stationary curves. However, the singular point at which the stationary points are annihilated does not always have the connection to the singular point in higher scale. Therefore, it is essential to find non-singular stationary points as the additional nodes of tree to which the annihilation points are connected. In this section, we firstly show that such nonsingular stationary points can be determined by tracing a unique figure flow curve from each singular point. Secondly, we introduce a *local minimum point at infinity* in order to define consistently the scale-space hierarchy. Finally, we propose the scale-space tree which explicitly describe the hierarchy. We briefly deal with

two-dimensional images to simplify the discussion.

### 3.2 Zero Principal Curvature Direction

Zhao and Iijima [4] showed that the stationary curves are the solutions of the system of linear equations:

$$\mathbf{H} \frac{d\mathbf{x}(\tau)}{d\tau} = -\nabla \Delta f(\mathbf{x}(\tau), \tau). \quad (9)$$

Equation (9) gives the velocity of the stationary points  $\mathbf{x}(\tau)$  in the space with respect to the scale. Transforming the coordinates into the principal axis coordinates of  $\mathbf{H}$ , we obtain from Eq. (9)

$$\frac{d\mathbf{p}(\tau)}{d\tau} = -\mathbf{A}^{-1} \nabla_{\mathbf{p}} \Delta f, \quad (10)$$

where  $\mathbf{p}(\tau) = \mathbf{V}^\top \mathbf{x}(\tau)$ , and  $\nabla_{\mathbf{p}}$  is the gradient operator in the principal axis coordinates.

Equation (10) shows that the third derivatives are weighted by the reciprocal eigenvalues. Recall that we have the zero eigenvalue of  $\mathbf{H}$  at the singular point. This indicates that the velocity component corresponding to the zero principal curvature becomes infinite at the singular point. In other words, the velocity of the stationary points is infinite in the direction of the zero principal curvature.

We observe the zero principal curvature directions at the annihilation points. Figure 1 illustrates the annihilation of local maximum and saddle. The annihilation point P is called a shoe point because of the shape of the surface [7, 9]. The shoe point has outward figure flow curves, but only one figure flow curve reaches the shoe point along the “instep” of the shoe. Here we call it “anti-directional figure flow curve”. The anti-directional figure flow curve connects another maximum point Q to the shoe point P. Therefore, we consider the point Q as the parent node of the annihilation point P.

It has been shown that generic annihilation events are described as Fold catastrophes [10, 11, 12]. The Fold catastrophe in the principal axis coordinates is modelled as

$$f(p_1, p_2, \tau) = p_1^3 + 6p_1\tau + \gamma(p_2^2 + 2\tau), \quad (11)$$

where  $\gamma = \pm 1$ . This model of scale-space image  $f(p_1, p_2, \tau)$  has a local maximum point and a saddle point if  $\tau < 0$  and  $\gamma = -1$ . These two stationary points meet at the origin at  $\tau = 0$ . A family of figure flow curves  $p_2 = C(p_1)$  are derived from the differential equation,

$$\frac{dp_2}{dp_1} = -\frac{\partial f / \partial p_2}{\partial f / \partial p_1}. \quad (12)$$

Figure 2 plots the figure flow curves before, after, and at the annihilation event of the local maximum point

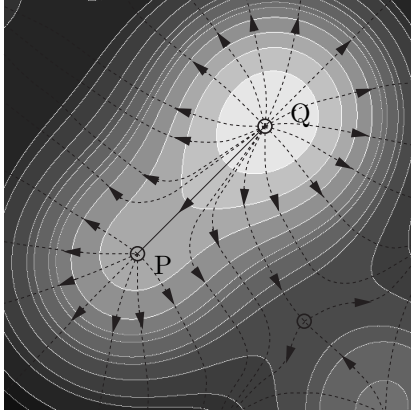


Figure 1: Figure flow around the shoe point. An anti-directional figure flow (solid line) penetrates into the shoe point P, which leads to a maximum point Q as the source of the flow.

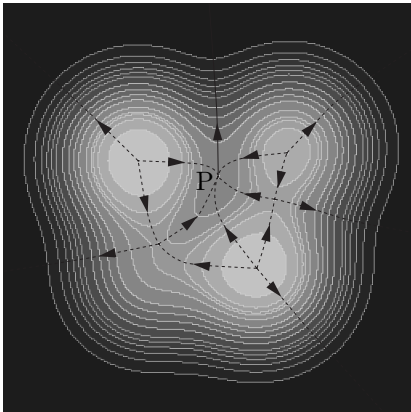


Figure 3: Figure flow around an annihilation point P of a local minimum point and a saddle point. In this example, the anti-directional figure flow (solid curve) from P does not have a drain in the region.

M and the saddle point S. We clearly see that the anti-directional figure flow curve coincides with the zero principal curvature direction, that is,  $p_1$ -axis.

However, we cannot always identify the stationary point as the parent of annihilation point in the finite domain of image. Figure 3 shows such a case of the annihilation event. The annihilation point P in Fig. 3 has inward figure flow curves, but only one outward figure flow curve is found as the anti-directional figure flow curve. The outward figure flow curve reaches the end of the region of image. This example suggests that the annihilation point like this case is linked to a drain of whole image intensity.

### 3.3 Stationary Point at Infinity

We conclude that the annihilation point of the local minimum in Fig. 3 is connected to a *point at infinity*. If the image function  $f(\mathbf{x}, \tau)$  is defined in the infinite domain, all of the outward figure flow curves from the whole region of the image are considered to converge at the point at infinity. Since the image function  $f(\mathbf{x}, \tau)$  is positive, the point at infinity is a drain, that is, the local minimum point. This local minimum point at infinity is representative of the dark background of the positive image. The local minimum point at infinity resides throughout the scale. We define the collection of local minimum points at infinity as the local minimum curve at infinity.

Furthermore, we presume that the local minimum point at infinity is annihilated with one remaining maximum point at infinite scale. This concept allows us to connect the remaining maximum curve to the local minimum curve at infinity. Consequently, the annihilation point is connected to the remaining maximum curve *through* the figure flow curve and the local minimum curve at infinity.

### 3.4 Scale-Space Tree

The hierarchical structure of image is described by a tree. The root of the tree is a virtual annihilation point of the local minimum point at infinity and remaining maximum point at infinite scale. The nodes of the tree are singular points. Stationary points which are connected to the annihilation points by the figure flow curves are also selected as the nodes of the tree. Some nodes may be the points at infinity. The leaves of the tree are the stationary points at the finest scale including the local minimum at infinity. The branches indicate the connections between the nodes by the stationary curves in the scale space and the figure flow curves. Thus, the figure field and stationary curves define the scale-space hierarchy.

## 4 Temporal Segmentation

### 4.1 Temporal Tree

The scale-space tree, which we define in the previous section, describes the hierarchical structure of the image. Suppose the image varies in time  $t$ , i.e. the motion image  $f(\mathbf{x}, t)$ . The hierarchical structure of the image can be expressed as the scale-space tree at any moment. If the image changes the structure with respect to time, we can detect the topological change of the scale-space tree. Thus, the motion image is divided into temporal segments by the variation of scale-space hierarchy.

We denote the algorithm for the construction of

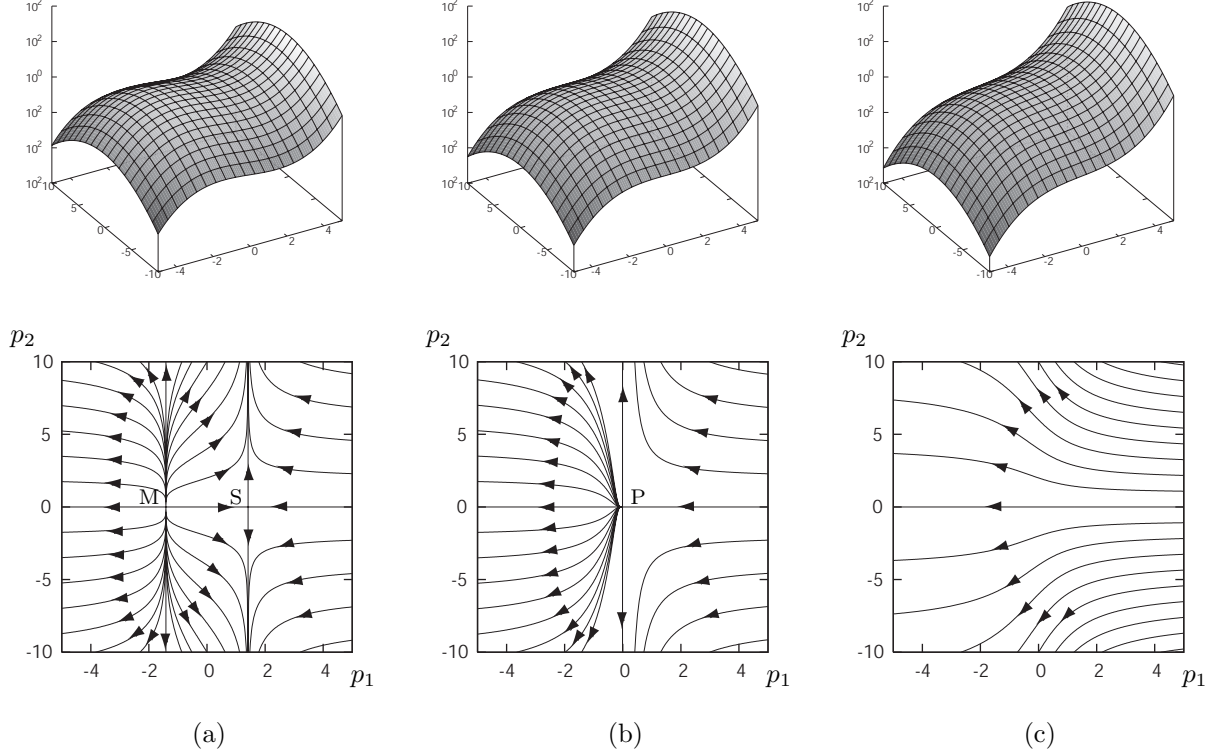


Figure 2: Surface plot of  $f(p_1, p_2)$  and corresponding figure flow curves (a) before, (b) at, and (c) after the Fold catastrophe event.

scale-space tree  $T(t)$  of the motion image by

$$\Theta(f(\mathbf{x}, t)) = T(t). \quad (13)$$

We call  $T(t)$  the temporal tree. In case that the motion image is given by a sequence of frame images  $f(\mathbf{x}, t_i)$ , The algorithm yields successive trees  $T(t_i)$ . If a pair of the successive trees  $T(t_i)$  ( $i_a \leq i \leq i_b$ ) are topologically equivalent, we represent the identical trees by  $T^{(i_a-i_b)}$ .

## 4.2 Approximated Tree Distance

For quantitative analysis of time-varying image with the temporal trees, we introduce a distance between the trees based on editing operations of the tree structure. Since it is possible to transform irregular trees to regular trees by adding dummy nodes “\*” to the irregular trees, our temporal trees can be assumed to be regular. Kawashima *et al.* have developed a method for a fast computation of the distance between regular rooted trees [13], which is applicable to the temporal trees.

Setting  $\alpha$  to be a  $k$ -digit number whose each digit is from 0 to  $k-1$ , the subtree of a node  $n_\alpha$  in the  $m$ -regular tree is expressed as

$$n_\alpha(T) = t_\alpha[T_{\alpha 1}, T_{\alpha 2}, \dots, T_{\alpha m}], \quad (14)$$

where  $t_\alpha$  is the label of the subtree rooted at the node  $n_\alpha$ , and  $T_{\alpha i}$  ( $i = 1, \dots, m$ ) is the subtree whose sub-

root is a child node of the node  $n_\alpha$ . Equation (14) expresses the whole tree for  $\alpha = 0$ , and  $n_0$  is the label of the root. Therefore,  $k$  is identical to the depth of the subtree.

The operations applied to the tree are replacement of a node label, permutation of subtrees, insertion of a subtree to “\*” and elimination of a subtree. These operations are respectively denoted by

$$\begin{aligned} E_r &: t_\alpha[T_{\alpha 1}, \dots, T_{\alpha m}] \\ &\rightarrow x_\alpha[T_{\alpha 1}, \dots, T_{\alpha m}], \end{aligned} \quad (15)$$

$$\begin{aligned} E_p &: t_\alpha[T_{\alpha 1}, \dots, T_{\alpha i}, \dots, T_{\alpha j}, \dots, T_{\alpha m}] \\ &\rightarrow t_\alpha[T_{\alpha 1}, \dots, T_{\alpha j}, \dots, T_{\alpha i}, \dots, T_{\alpha m}], \end{aligned} \quad (16)$$

$$\begin{aligned} E_i(S) &: t_\alpha[T_{\alpha 1}, \dots, *, \dots, T_{\alpha m}] \\ &\rightarrow t_\alpha[T_{\alpha 1}, \dots, S, \dots, T_{\alpha m}], \end{aligned} \quad (17)$$

$$\begin{aligned} E_e(T_{\alpha k}) &: t_\alpha[T_{\alpha 1}, \dots, T_{\alpha k}, \dots, T_{\alpha m}] \\ &\rightarrow t_\alpha[T_{\alpha 1}, \dots, *, \dots, T_{\alpha m}]. \end{aligned} \quad (18)$$

For these operations, the lengths of operations are defined as:

$$d(s_\alpha) = \frac{1}{1+l_\alpha} |s_\alpha|. \quad (19)$$

Here,

$$l_\alpha = \begin{cases} 0, & \text{if } \alpha = 0, \\ \text{the number of digits of } \alpha, & \text{otherwise,} \end{cases} \quad (20)$$

and

$$|s_\alpha| = \begin{cases} 0, & \text{if } s_\alpha \text{ is nonoperation,} \\ 1, & \text{if } s_\alpha \text{ is the replacement } E_r, \\ |P|, & \text{if } s_\alpha \text{ is the permutation } E_p, \\ |S|, & \text{if } s_\alpha \text{ is the insertion } E_i, \\ |S|, & \text{if } s_\alpha \text{ is the elimination } E_e, \end{cases} \quad (21)$$

where  $|P|$  is the number of the permutations. The distance between trees  $T$  and  $T'$  is defined as the sum of lengths:

$$D(T, T') = \sum_{\alpha=1}^n d(s_\alpha) \quad (22)$$

for the sequence of operations  $\{s_1, s_2, \dots, s_n\}$  which transforms  $T$  to  $T'$ . This tree distance satisfies the following lemma.

**Lemma 1.** *The distance in eq. (22) is metric for trees with almost same order, that is, it satisfies the conditions of distance.*

*Proof.* It is obvious that  $D(T, T) = 0$  and that  $D(T, T') = D(T', T)$ . Setting

$$\{s_1, s_2, \dots, s_n\}, \{t_1, t_2, \dots, t_n\}, \{u_1, u_2, \dots, u_n\} \quad (23)$$

to be sequences of transformation from  $T$  to  $T'$ , from  $T'$  to  $T''$  and from  $T''$  to  $T$  for a triplet of almost same size trees, we obtain the relation

$$|s_k| + |t_k| \geq |u_k|. \quad (24)$$

This derives the relation

$$D(T, T') + D(T', T'') \geq D(T, T'').$$

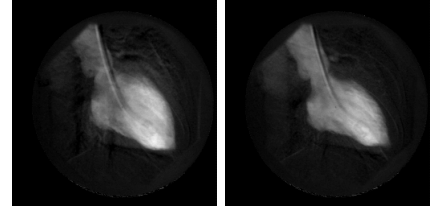
□

## 5 Application

We apply the temporal segmentation to a sequence of beating heart images [15]. Figure 1 shows the 1st, 6th, 7th, 8th, 11th, 12th, 32nd, 33rd and the 38th frame from 38 frames of the sequence.

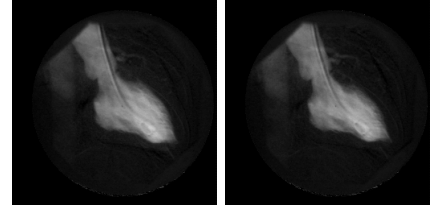
Figure 2 shows the stationary curves of these frames of the beating heart. The temporal tree analysis detects topological difference between the 6th and 7th, 7th and 8th, 11th and 12th, 12th and 13th, 31st and 32nd and between the 32nd and 33rd frames. No topological transition is found between the other two successive images. Thus the image sequence of beating heart is segmented into seven groups of frames: the 1st to 6th frames, the 7th frame, the 8th to 11th frames, the 12th frame, the 13th to 31st frames, the 32nd frame and the 33rd to 38th frame. Corresponding temporal trees are shown in Figure 3. The distances among trees with topological difference are

$$\begin{aligned} D(T(6), T(7)) &= 1.5, & D(T(7), T(8)) &= 3, \\ D(T(11), T(12)) &= 3, & D(T(12), T(13)) &= 1.5, \\ D(T(31), T(32)) &= 1.5, & D(T(32), T(33)) &= 1.5. \end{aligned}$$



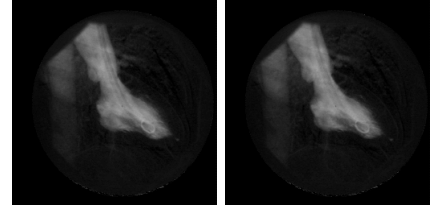
(a)

(b)



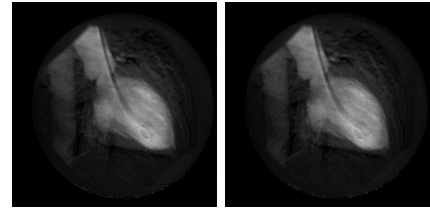
(c)

(d)



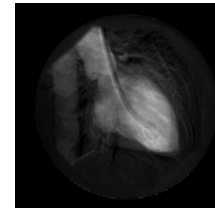
(e)

(f)



(g)

(h)



(i)

Figure 4: Sequence of beating heart. The images from (a) to (i) are the 1st, 6th, 7th, 8th, 11th, 12th, 32nd, 33rd and the 38th frame from 38 frames, respectively. The topology of the temporal tree changes before and after these images.

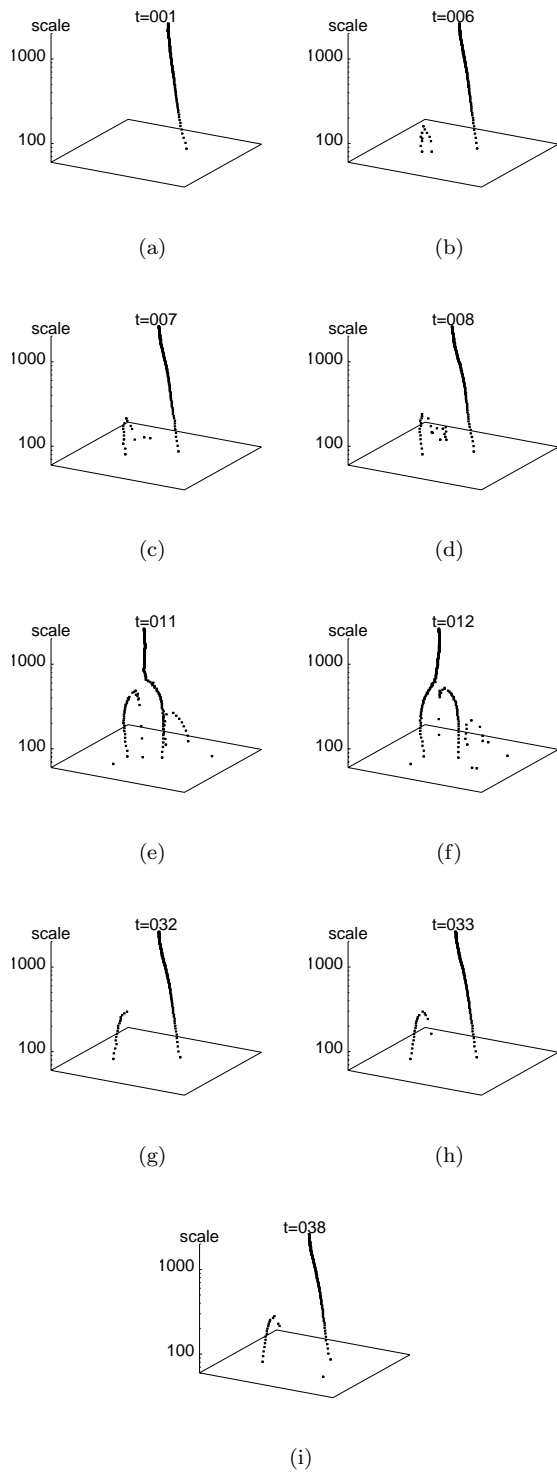


Figure 5: Sequence of stationary curves of beating heart, corresponding to the images in Figure 1. The scale axis is in log scale.

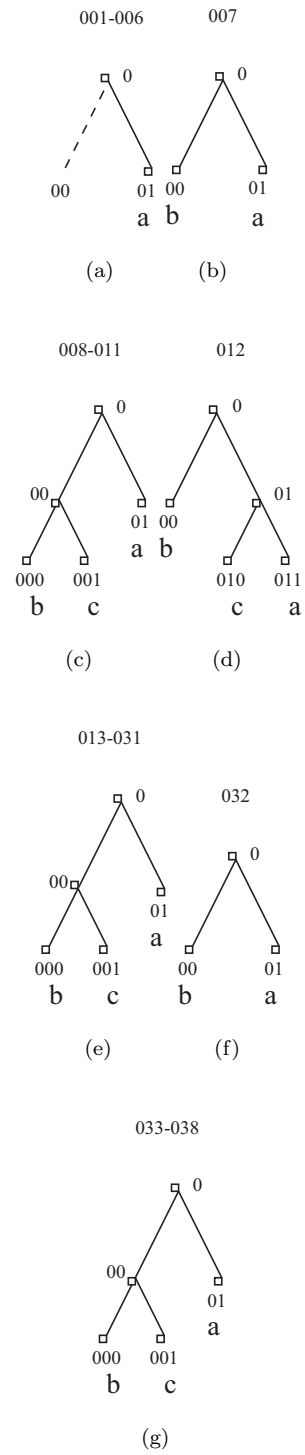


Figure 6: Temporal trees of the sequence of beating heart. (a) Tree of from the 1st to 6th. (b) Tree of the 7th. (c) Tree of from the 8th to 11th. (d) Tree of the 12th. (e) Tree of from the 13th to 31st. (f) Tree of 32nd. (g) Tree of from the 33rd to 38th. These trees symbolize the hierarchical structures of the images.

The temporal scale space analysis achieves the detection of topological changes of beating heart. The result indicates that our temporal scale-space analysis based on tree construction in the scale space is feasible to the sequential analysis of low-contrast medical images as this example.

## 6 Conclusions

Firstly, we developed a method to construct the scale-space tree which qualitatively describes the hierarchical structure of a greyscale image. The scale-space tree has two types of nodes: singular points and additional local extrema. The local extrema selected as the nodes are linked to the annihilation points by the figure flow curves, of which directions coincide with the zero principal curvature directions at the annihilation points.

Secondly, the temporal segmentation of the motion image is achieved by detecting the topological changes of the temporal tree. We applied the temporal segmentation to the motion image of beating heart. The sequence of images is segmented into groups based on the structures of frame images. Our temporal segmentation scheme is non-heuristic, non-model-based, and is performed without any quantitative estimation such as edge extraction, motion detection, etc.

## References

- [1] Iijima, T., *Basic theory on the normalization of two-dimensional visual pattern*, Studies on Information and Control, Pattern Recognition Issue, IEICE Japan, 1, 15-22, 1963 (in Japanese).
- [2] Witkin, A.P., *Scale space filtering*, Proc. of 8th IJCAI, 1019-1022, 1983.
- [3] Koenderink, J. J., *The structure of images*, Biological Cybernetics, 50, 363-370, 1984.
- [4] Zhao, N.-Y., Iijima, T., *Theory on the method of determination of view-point and field of vision during observation and measurement of figure*, IEICE Japan, Trans. D., J68-D, 508-514, 1985 (in Japanese).
- [5] Zhao, N.-Y., Iijima, T., *A theory of feature extraction by the tree of stable view-points*. IEICE Japan, Trans. D., J68-D, 1125-1135, 1985 (in Japanese).
- [6] Weickert, J., Ishikawa, S., Imiya, A., *Linear Scale-Space has First been Proposed in Japan*, Journal of Mathematical Imaging and Vision, 10, 237-252, 1999.
- [7] Griffin, L. D., Colchester, A., *Superficial and deep structure in linear diffusion scale space: Isophotes, critical points and separatrices*, Image and Vision Computing, 13, 7, 543-557, 1995.
- [8] Kuijper, A., Florack, L.M.J., Viergever, M.A., *Scale Space Hierarchy*, Journal of Mathematical Imaging and Vision, 18-2, 169-189, 2003.
- [9] Olsen, O.F., Nielsen, M., *Generic events for the gradient squared with application to multi-scale segmentation*, LNCS, 1252, 101-112, 1997.
- [10] Kuijper, A., *The deep structure of Gaussian scale-space images*, PhD thesis, Utrecht University, 2002.
- [11] Damon, J., *Local Morse Theory for Solutions to the Heat Equation and Gaussian Blurring*, Journal of Differential Equations, 115, 368-401, 1995.
- [12] Damon, J., *Generic Properties of Solutions to Partial Differential Equations*, Arch. Rational Mech. Anal., 140, 353-403, 1997.
- [13] Kawashima, T., Imiya, A., Nishida, F., *Approximate tree distance*, Technical Report of IEICE, PRMU96-36, 81-87, 1996.
- [14] Lindeberg, T., *Scale-Space Theory in Computer Vision*, Kluwer, Boston 1994.
- [15] <http://sampl.eng.ohio-state.edu/~sampl/data/motion/Heart/index.htm>